Structural Characteristics and Catalytic Properties of Highly Dispersed ZrO₂/SiO₂ and V₂O₅/ZrO₂/SiO₂ Catalysts

Xingtao Gao,[†] J. L. G. Fierro,[‡] and Israel E. Wachs*,[†]

Department of Chemistry and Chemical Engineering, Zettlemoyer Center for Surface Studies, Lehigh University, 7 Asa Drive, Bethlehem, Pennsylvania 18015, and Institute de Catalisis y Petroleoquimica, CSIC, Campus Univeritario Cantoblanco, E-28049 Madrid, Spain

Highly dispersed ZrO₂/SiO₂ and V₂O₅/ZrO₂/SiO₂ catalysts were successfully synthesized by the incipient wetness impregnation method. The surface structures of these catalysts in hydrated and dehydrated states were characterized by in situ Raman and UV−vis−near-infrared diffuse reflectance spectroscopies. Temperature-programmed reduction and methanol oxidation were employed as chemical probe reactions to examine the reducibility and reactivity/selectivity properties of these catalysts. These characterization techniques demonstrate that both zirconium oxide and vanadium oxide species are highly dispersed as two-dimensional metal oxide overlayers on the silica support. The spectroscopic results revealed that the surface vanadium oxide species on the highly dispersed ZrO₂/SiO₂ supports are predominantly isolated VO₄ units [O=V(O−support)₃] in the dehydrated state and become polymerized vanadium oxide species upon hydration. The surface vanadium oxide species preferentially interact with the zirconium oxide species on the silica surface. The substitution of Si^{IV}−O$^-$ by Zr^{IV}−O$^-$ ligands significantly affects the chemical properties of the isolated VO₄ units: the reducibility of the surface vanadium oxide species increases, and the methanol oxidation turnover frequency (TOF) increases by 1−2 orders of magnitude relative to V₂O₅/SiO₂. The present study demonstrates that the support effect, variation in the reactivity of supported metal oxide catalysts due to different oxide supports, essentially originates from the difference in oxygenated ligands around the active metal cations.

Introduction

Zirconia−silica materials have attracted much attention in recent years because of their interesting properties for applications in heterogeneous catalysis,[1−4] photocatalysis,[5] and ceramic glasses.[6−9] ZrO₂−SiO₂ mixed oxides are very important materials with excellent chemical resistance to alkaline corrosion and low thermal expansions.[6−9] ZrO₂−SiO₂ mixed oxides display strong surface acidity and have been applied for reactions including alcohol dehydration,[1,3] alkene isomerization,[2] and cumene dealkylation.[3] ZrO₂/SiO₂-supported oxides exhibit hydrogenation activity and have been tested in propene hydrogenation.[10]

Pure zirconia exhibits catalytic activity in a number of reactions, including hydrogenation,[11] dehydrogenation,[12] selective formation of isobutane and isobutene from synthesis gas,[13] and cracking and alcohol dehydration to alkenes.[14] This is because zirconia possesses both acidic and basic surface sites as well as both oxidizing and reducing characteristics.[15] Zirconia is also an excellent active support material for various oxidation reactions, including methanol oxidation, CO oxidation and selective catalytic reduction (SCR) of NO$_x$ with NH₃.[16] Therefore, ZrO₂/SiO₂-supported oxides have been considered as potentially improved support materials to substitute pure ZrO₂ because they combine the favorable chemical properties of zirconia with the high surface area and excellent thermal/mechanical stability of silica and are more economically attractive.[17,18]

The highly dispersed ZrO₂/SiO₂-supported oxides are usually prepared by the surface reaction of Si−OH hydroxyls with Zr ethoxide[17] and Zr propoxide.[10,18] In the present study, a very reactive H-sequestering reagent, Zr *tert*-butoxide, was used to prepare the highly dispersed ZrO₂/SiO₂-supported oxides. The dispersion and surface structure of dispersed zirconium oxide species on silica were investigated by Raman spectroscopy, X-ray photoelectron spectroscopy (XPS), and UV−vis−near-infrared (NIR) diffuse reflectance spectroscopy (DRS). Moreover, the catalytic properties of the highly dispersed ZrO₂/SiO₂ catalysts were examined using methanol oxidation as a chemical probe reaction.

Although dispersed ZrO₂/SiO₂-supported oxides have been considered as advanced support materials, no fundamental studies have been done to investigate the nature of the interaction between active species and the zirconium surface modified supports. In the present work,

* To whom correspondence should be addressed.

† Lehigh University. E-mail: xig2@lehigh.edu and iew0@lehigh.edu.

‡ CSIC.

(1) Bosman, H. J. M.; Kruissink, E. C.; van der Spoel, J.; van den Brink, F. *J. Catal.* **1994**, *148*, 660.

(2) (a) Miller, J. B.; Rankin, S. E.; Ko, E. I. *J. Catal.* **1994**, *148*, 673. (b) Miller, J. B.; Ko, E. I. *J. Catal.* **1995**, *153*, 194. (c) Miller, J. B.; Ko, E. I. *Chem. Eng. J.* **1996**, *64*, 273.

(3) Sohn, J. R.; Jang, H. J. *J. Mol. Catal.* **1991**, *64*, 349.

(4) Fisher, I. A.; Woo, H. C.; Bell, A. T. *Catal. Lett.* **1997**, *44*, 11.

(5) Moon, S.-C.; Fujino, M.; Yamashita, H.; Anpo, M. *J. Phys. Chem. B* **1997**, *101*, 369.

(6) Stachs, O.; Petkov, V.; Gerber, T. *J. Appl. Crystallogr.* **1997**, *30*, 670.

(7) Okasaka, K.; Nasu, H.; Kamiya, K. *J. Non-Cryst. Solids* **1991**, *136*, 103.

(8) Nogami, M. *J. Non-Cryst. Solids* **1985**, *69*, 415.

(9) Li, X.; Johnson, P. *Mater. Res. Soc. Proc.* **1990**, *180*, 335.

(10) Naito, S.; Tanimoto, M. *J. Catal.* **1995**, *154*, 306.

(11) Tanabe, K.; Yamagushi, T. *Catal. Today* **1994**, *20*, 185.

(12) Davis, B. H. *J. Catal.* **1983**, *79*, 58.

(13) Feng, Z.; Postula, W. S.; Erkey, C.; Philip, C. V.; Akgerman, A.; Anthony, R. G. *J. Catal.* **1994**, *148*, 84.

(14) Yamagushi, T.; Sasaki, H.; Tanabe, K. *Chem. Lett.* **1973**, 1017.

(15) Tanabe, K. *Mater. Chem. Phys.* **1985**, *13*, 347.

(16) Deo, G.; Wachs, I. E.; Haber, J. *Crit. Rev. Surf. Chem.* **1994**, *4*, 141.

(17) Meijers, A. C. Q. M.; de Jong, A. M.; van Gruijthuijsen, L. M. P.; Niemantsverdriet, J. W. *Appl. Catal.* **1991**, *70*, 53.

(18) Damyanova, S.; Grange, P.; Delmon, B. *J. Catal.* **1997**, *168*, 421.

a series of highly dispersed $V_2O_5/ZrO_2/SiO_2$ samples were prepared as model catalysts for understanding the interfacial interactions between surface vanadium oxide and zirconium oxide on silica. The molecular structures of the highly dispersed $V_2O_5/ZrO_2/SiO_2$ catalysts under various conditions (e.g., hydration, dehydration) were extensively investigated by employing in situ Raman spectroscopy as well as UV−vis−NIR DRS spectroscopy. Methanol oxidation was used as a chemical probe reaction to examine the catalytic properties of the $V_2O_5/ZrO_2/SiO_2$ catalysts. In addition, temperature-programmed reduction (TPR) was used to examine their redox properties. The results from these studies allow us to establish the fundamental relationships between structural characteristics and the reactivity/selectivity properties of this catalyst system and provide an important understanding about how to molecularly engineer supported metal oxide catalysts by modifying the oxide support material.

Experimental Section

1. Catalyst Preparation. The silica support was Cabosil EH-5. This fluffy material was treated with water to condense its volume for easier handling. The wet SiO_2 was dried at 120 °C and subsequently calcined at 500 °C overnight. The resulting surface area was 332 m^2/g.

The ZrO_2/SiO_2-supported oxide catalysts were prepared by the incipient-wetness impregnation of toluene solutions of zirconium *tert*-butoxide (Alfa-Aesar, 98% purity). The preparation was performed inside a glovebox with continuously flowing N_2. The SiO_2 support was initially dried at 120 °C to remove the physisorbed water before impregnation. After impregnation, the samples were kept inside the glovebox overnight. The samples were subsequently dried at 120 °C in flowing N_2 for 1 h and calcined at 500 °C in flowing air for 4 h. A two-step preparation procedure was employed to prepare the 10% and 15% ZrO_2/SiO_2 samples, where the second impregnation followed the same procedure described above by using 8% ZrO_2/SiO_2 as the starting material. The final catalysts were denoted as x% ZrO_2/SiO_2. Pure ZrO_2 (Degussa, S_{BET} = 34 m^2/g) was used for comparison.

The supported vanadium oxide catalysts were prepared by the incipient-wetness impregnation of 2-propanol solutions of vanadium isopropoxide ($VO(O-Pr^i)_3$, Alfa-Aesar, 97% purity) with various oxide supports (SiO_2, ZrO_2, and ZrO_2/SiO_2). The preparation was performed inside a glovebox. The support materials were dried at 120 °C before impregnation. After impregnation, the samples were kept inside the glovebox with flowing N_2 overnight. The samples were subsequently dried in flowing N_2 at 120 °C for 1 h and 300 °C for 1 h. The $V_2O_5/ZrO_2/SiO_2$ samples were further calcined in flowing air at 300 °C for 1 h and 500 °C for 2 h, while the V_2O_5/SiO_2 and V_2O_5/ZrO_2 samples were calcined in flowing air at 300 °C for 1 h and 450 °C for 2 h.

2. Raman Spectroscopy. The Raman spectra were obtained with the 514.5 nm line of an Ar^+ ion laser (Spectra Physics, model 164). The scattered radiation from the sample was directed into an OMA III (Princeton Applied Research, model 1463) optical multichannel analyzer with a photodiode array cooled thermoelectrically to −35 °C. The samples were pressed into self-supporting wafers. The Raman spectra of the hydrated samples were collected during rotation of the sample under ambient conditions. The Raman spectra of the dehydrated samples were recorded at room temperature after heating the sample in flowing O_2 at 450−500 °C for 1 h in a stationary quartz cell.

3. XPS. XPS spectra were collected with a Fisons ESCALAB 200R electron spectrometer equipped with a hemispherical electron analyzer and a Mg Kα X-ray source ($h\nu$ = 1253.6 eV) powered at 120 W. The samples were placed in small copper cylinders and mounted on a transfer rod placed in the pretreatment chamber of the instrument. All samples were outgassed at 200 °C before XPS analysis. The binding energies (BE) were referenced to Si 2p (BE = 103.4 eV) with an accuracy of ±0.2 eV. The atomic concentration ratios were calculated by correcting the intensity ratios with theoretical sensitivity factors proposed by the manufacturer.

Table 1. Binding Energies and Surface Compositions of the ZrO₂/SiO₂ Samples

sample	Si 2p (eV)	Zr 3d$_{5/2}$ (eV)	O 1s (eV)	Zr/Si atomic ratio
1% ZrO₂/SiO₂	103.4	182.3	532.9	0.021
5% ZrO₂/SiO₂	103.4	182.2	532.9 (92)[a] 530.7 (8)	0.044
10% ZrO₂/SiO₂	103.4	182.2	532.9 (88) 530.5 (12)	0.084
15% ZrO₂/SiO₂	103.4	182.2	532.9 (82) 530.5 (18)	0.193

[a] The numbers in parentheses indicate the percentage of the band.

4. UV−Vis−NIR DRS. DRS spectra in the range of 200−2200 nm were taken on a Varian Cary 5 UV−vis−NIR spectrophotometer. The spectra were recorded against a halon white reflectance standard as the baseline. The computer processing of the spectra with Bio-Rad Win-IR software consisted of calculation of the Kubelka−Munk function ($F(R_\infty)$) from the absorbance. The band-gap energy (E_g) for allowed transitions was determined by finding the intercept of the straight line in the low energy rise of a plot of $[F(R_\infty) \times h\nu]^2$ against $h\nu$, where $h\nu$ is the incident photon energy.[19] Samples were loaded in a quartz flow cell with a Suprasil window. The spectra of the hydrated samples were obtained under ambient conditions. The spectra of the dehydrated samples were obtained after samples were calcined at 500 °C in flowing O_2/He for 1 h.

5. TPR. TPR was carried out with an AMI-100 system (Zeton Altamira Instruments). The catalyst sample (~60 mg) was loaded in a U-type quartz tube and pretreated at 500 °C in flowing dry air for 1 h. The temperature was then ramped from 150 to 700 °C with a constant heating rate of 10 °C in 10% H_2/Ar with a flow rate of 30 mL/min. An on-line thermal conductivity detector (TCD) was used to record the H_2 consumption, and CuO was used to verify the calibration of the instrument (the experimental error is within 10%).

6. Methanol Oxidation. The reaction was carried out in an isothermal fixed-bed differential reactor. 12−60 mg of catalyst with a size fraction of 60−100 mesh was tested for methanol oxidation at various temperatures at atmospheric pressure. The reactant gas mixture of $CH_3OH/O_2/He$, with a molar ratio of ~6/13/81, was used with a total flow rate of 100 mL/min. Analysis of the reactor effluent was performed using an on-line gas chromatograph (HP 5890 series II) equipped with flame ionization and thermal conductivity detectors (FID and TCD). A Carboxene-1000 packed column and a CP-sil 5CB capillary column were used in parallel for TCD and FID, respectively. The samples were pretreated in a stream of O_2/He gas mixture at 450 °C for 0.5 h before each run, and the activity and selectivity data were obtained for catalytic runs within 2 h.

Results

1. XPS Surface Analysis of the ZrO₂/SiO₂ Samples. The Zr/Si surface atomic ratios of the dehydrated ZrO_2/SiO_2 samples obtained by the XPS analysis are listed in Table 1 and are plotted as a function of zirconia loading in Figure 1. The Zr/Si surface ratios vary approximately linearly with the zirconia loading, suggesting that the zirconium oxide on the silica surface may be highly dispersed.

The BE values of Zr 3d$_{5/2}$ and O 1s for the dehydrated ZrO_2/SiO_2 samples are also listed in Table 1. With the BE of Si 2p as the internal reference, the BE of Zr 3d$_{5/2}$ is almost constant at ~182.2 eV, indicating that the Zr cations are in an oxidation state of +4.[17] The BE of O 1s in pure silica is ~533.0 eV. A new O 1s peak appears at a lower binding energy of ~530.5 eV at zirconia loadings of 5% ZrO_2 and above. The relative percentage of this new

(19) Delgass, W. N.; Haller, G. L.; Kellerman, R.; Lunsford, J. H. *Spectroscopy in Heterogeneous Catalysis*; Academic Press: New York, 1979.
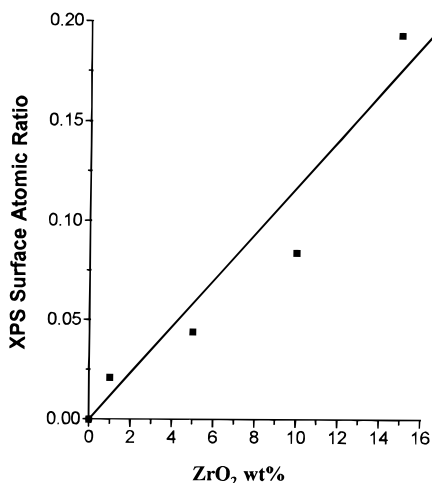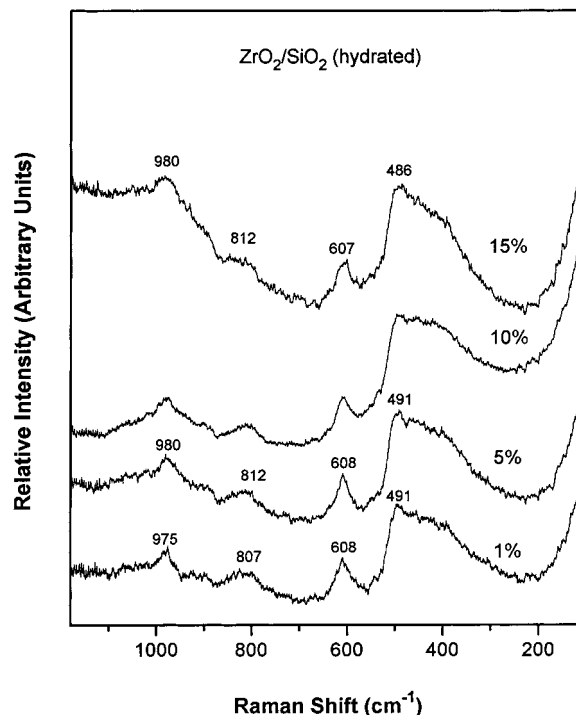
Figure 1. Zr/Si XPS surface atomic ratio as a function of the ZrO_2 loading.
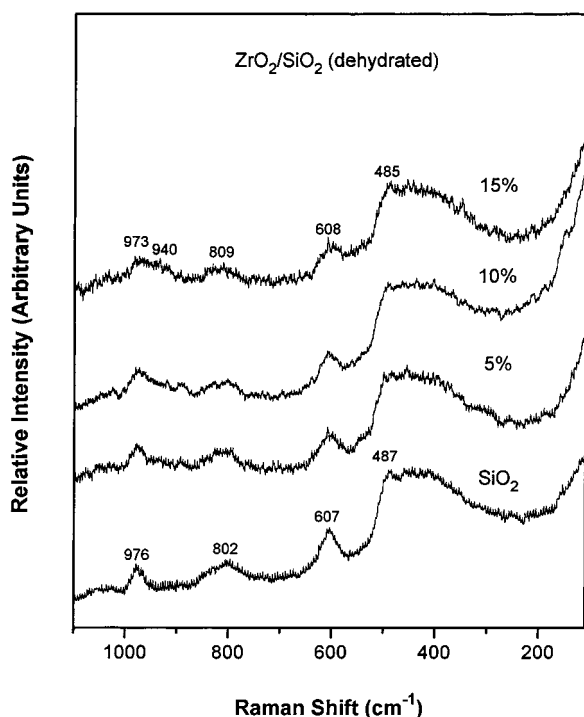
Figure 2. Raman spectra of the dehydrated ZrO_2/SiO_2 samples.

Figure 3. Raman spectra of the hydrated ZrO_2/SiO_2 samples.

O 1s increases with zirconia loading, suggesting that this new O 1s peak is associated with the dispersed zirconium oxide species on the silica support.

2. Raman Spectroscopy. The Raman spectra of the dehydrated ZrO_2/SiO_2 samples are presented in Figure 2. The silica support possesses Raman features at ~410, ~487, 607, 802, and ~976 cm^{-1}. No significant spectral change can be seen upon the deposition of zirconium oxide species onto the silica surface. The 976 cm^{-1} band due to the Si–OH stretching vibration[20] appears to be broadened toward the lower wavenumber side with increasing zirconia loading, and a weak Raman band appears at ~940 cm^{-1}. For ZrO_2–SiO_2 glasses, broad Raman bands observed at ~976 and ~954 cm^{-1} have been assigned to Si–O–H and Si–O–Zr linkages, respectively.[21] Thus, it

appears that the deposition of zirconium oxide species on the silica surface may form some Si–O–Zr bridging bonds. However, no Raman bands at 280, 316, 462, and 644 cm^{-1} due to tetragonal ZrO_2,[24] at 614 and 637 cm^{-1} due to monoclinic ZrO_2,[25] and at ~230, 360, 450, and 975 cm^{-1} due to zircon ($ZrSiO_4$)[21] are observed on these ZrO_2/SiO_2 samples. Also, no Raman bands at 148, 263, 476, and 550 cm^{-1} due to three-dimensional amorphous zirconia[26] and at 550 cm^{-1} due to cubic zirconia-type ZrO_8 units in ZrO_2–SiO_2 glasses[21] are detected. The Raman results indicate that the zirconium oxide species on silica are amorphous in nature and are probably present as highly dispersed surface species.

Upon hydration, the Raman band centered at 975–980 cm^{-1} becomes broader and stronger in the 1100–900 cm^{-1} region with increasing zirconia loading for the ZrO_2/SiO_2 samples relative to the silica support (see Figure 3). The broadening of this Raman band may be associated with the formation of Zr–OH hydroxyls and more Si–OH hydroxyls the Zr–OH hydroxyls display a Raman band at ~1050 cm^{-1} [22] and the Si–OH hydroxyls perturbed by nearby metal cations tend to exhibit Raman bands at lower wavenumbers than nonperturbed hydroxyls.[23] These results suggest that some Si–OH and Zr–OH hydroxyls are generated from the hydrolysis of the Si–O–Zr bonds.

The Raman spectra of the dehydrated 10% V_2O_5 on 0–15% ZrO_2/SiO_2 supports are compared in Figure 4. No V_2O_5 crystallites are detected on these samples because no Raman bands appear at 994, 697, 284, and 144 cm^{-1} due to crystalline V_2O_5. The dehydrated 10% V_2O_5/SiO_2 sample possesses a Raman sharp band at 1041 cm^{-1} from the terminal V=O vibration of the isolated VO_4 species

(20) (a) Tallant, D. R.; Bunker, B. C.; Brinker, C. J.; Balfe, C. A. *Mater. Res. Soc. Symp. Proc.* **1986**, *73*, 261. (b) Stolen, R. H.; Walrafen, G. E. *J. Chem. Phys.* **1976**, *64*, 2623. (c) Brinker, C. J.; Tallant, D. R.; Roth, E. P.; Ashley, C. S. *Mater. Res. Soc. Symp. Proc.* **1986**, *61*, 387.
(21) Lee, S. W.; Condrate, R. A., Sr. *J. Mater. Sci.* **1988**, *23*, 2951.

(22) Roozeboom, F.; Mitteimeijer-Hazeleger, M. C.; Moulljn, J. A.; Medema, J.; de Beer, V. H. J.; Gellings, P. J. *J. Phys. Chem.* **1980**, *84*, 2783.
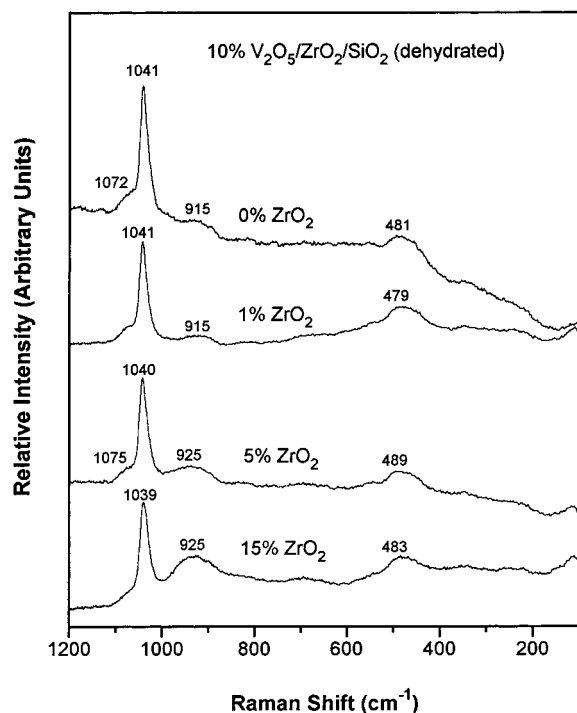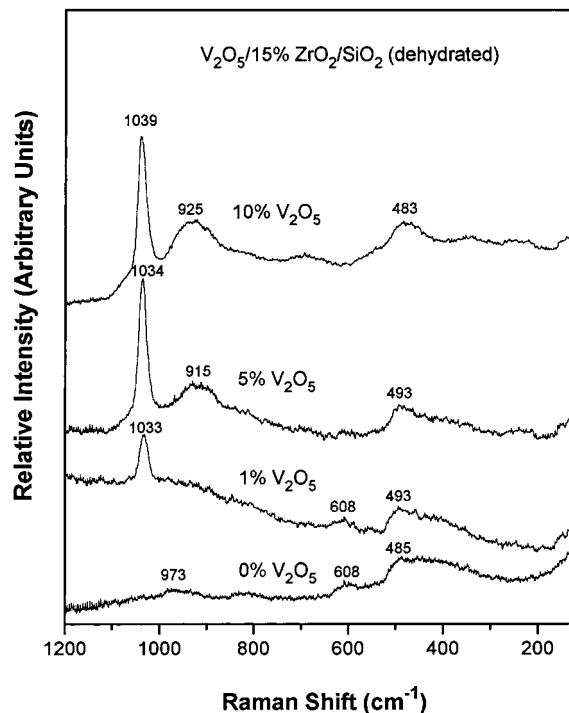(23) Gao, X.; Bare, S. R.; Fierro, J. L. G.; Banares, M. A.; Wachs, I. E. *J. Phys. Chem. B* **1998**, *102*, 5653.
(24) Arash, H.; Ishigame, M. *Phys. Status Solidi A* **1982**, *71*, 313.
(25) Anastassakis, E.; Papanicolaou, B.; Asher, I. M. *J. Phys. Chem. Solids* **1975**, *36*, 667.
(26) Keramidas, V. G.; White, W. B. *J. Am. Ceram. Soc.* **1974**, *57*, 22.

Figure 4. Raman spectra of the dehydrated 10% $V_2O_5/ZrO_2/$ SiO_2 samples.

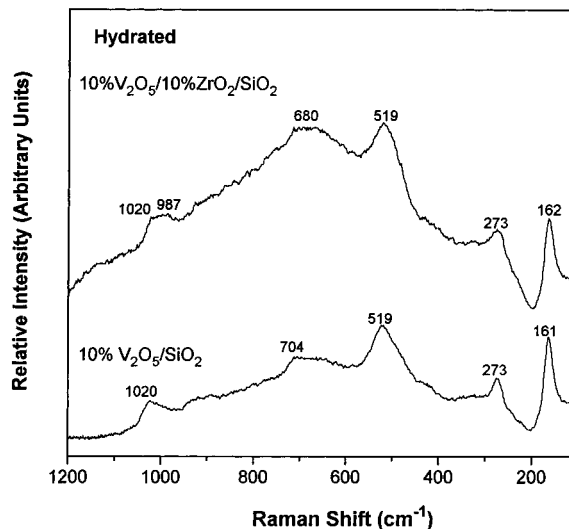**Figure 5.** Raman spectra of the dehydrated $V_2O_5/15\%$ $ZrO_2/$ SiO_2 samples.

and weaker bands at 1072, 915, and 481 cm^{-1} due to silica vibrations.[27] The Raman spectra of the 10%$V_2O_5/ZrO_2/$ SiO_2 samples are very similar to that of the 10% $V_2O_5/$ SiO_2 sample with the exception of the 915–930 cm^{-1} band. Increasing the zirconia loading shifts the Raman band from 915 to 925 cm^{-1} and increases its relative intensity. The Raman band at 840–940 cm^{-1} for the dehydrated V_2O_5/ZrO_2 samples has been assigned to polymerized surface V–O–V species.[16] However, no apparent additional Raman bands at 200–300 cm^{-1} due to the corresponding bending mode of the polymerized V–O–V species[30] are observed. Additional information from other characterization techniques is necessary to clarify the identity of this 915–930 cm^{-1} Raman band (see the next section).

The Raman spectra of the dehydrated 0–10% $V_2O_5/$ 15%ZrO_2/SiO_2 samples are presented in Figure 5. A strong band at 1033–1039 cm^{-1} due to the V=O stretching vibration appears upon the deposition of vanadium oxide. Unlike the dehydrated, highly dispersed V_2O_5/SiO_2 samples whose V=O vibration is independent of vanadia loading at ~1040 cm^{-1},[27] decreasing the vanadia loading on the ZrO_2/SiO_2 support shifts the V=O vibration to lower wavenumbers. The 607 cm^{-1} band, due to the three-membered siloxane rings,[28,29] decreases with increasing vanadia loading, indicating that the silica surface covered with the zirconium oxide species also interacts with the surface vanadium oxide species. Notably, a broad Raman band appears at ~915 cm^{-1} for the 5% $V_2O_5/15\%$ $ZrO_2/$ SiO_2 sample, becomes more intense, and shifts to ~925 cm^{-1} for the 10% $V_2O_5/15\%$ ZrO_2/SiO_2 sample.

The Raman spectra of the hydrated 10% V_2O_5/SiO_2 and 10% $V_2O_5/10\%$ ZrO_2/SiO_2 samples are shown in Figure 6.

(27) Gao, X.; Bare, S. R.; Weckhuysen, B. M.; Wachs, I. E. *J. Phys. Chem. B* **1998**, *102*, 10842.

(28) Brinker, C. J.; Kirkpatrick, R. J.; Tallant, D. R.; Bunker, B. C.; Montez, B. *J. Non-Cryst. Solids* **1988**, *99*, 418.

(29) Morrow, B. A.; Mcfarlan, A. J. *J. Non-Cryst. Solids* **1990**, *120*, 61.

(30) Deo, G. Ph.D. Thesis, Lehigh University, Bethlehem, PA, 1992.

Figure 6. Comparison of Raman spectra of the hydrated 10% V_2O_5/SiO_2 and 10% $V_2O_5/10\%$ ZrO_2/SiO_2 samples.

These spectra are very similar, suggesting that the molecular structure of the hydrated surface vanadium oxide species on pure SiO_2 and 10% ZrO_2/SiO_2 are similar. The Raman bands observed at ~1020, 704–650, ~518, 273–264, and 164–155 cm^{-1} for the hydrated V_2O_5/SiO_2 catalysts are due to polymerized VO_5/VO_6 species.[27] Thus, the Raman results suggest that the polymerized VO_5/VO_6 species probably also dominate on the hydrated ZrO_2/SiO_2 supports.
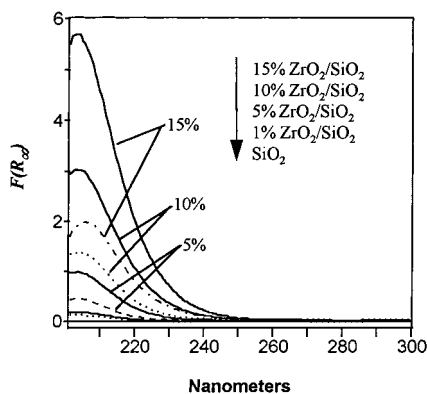
3. UV–Vis–NIR DRS. The UV–vis DRS spectra of the hydrated and dehydrated 1–15% ZrO_2/SiO_2 samples are provided in Figure 7, and the corresponding band maxima and edge energies of the ligand-to-metal charge-transfer (LMCT) transitions of the Zr cations are listed in Table 2. The band maxima and edge energies of these ZrO_2/SiO_2 samples are located within 203–205 nm and 5.74–5.64 eV, respectively, regardless of zirconia loading and environmental conditions. However, the absorption

Figure 7. UV−vis DRS spectra of the hydrated (dashed lines) and dehydrated (solid lines) ZrO₂/SiO₂ samples.

Table 2. Band Maxima and Edge Energies of the ZrO₂/SiO₂ Samples under Hydrated and Dehydrated Conditions

sample	band max (nm) (dehy)	E_g (eV) (dehy)	band max (nm) (hydr)	E_g (eV) (hydr)
1% ZrO₂/SiO₂	204	5.69	204	5.72
5% ZrO₂/SiO₂	204	5.70	204	5.74
10% ZrO₂/SiO₂	203	5.67	204	5.68
15% ZrO₂/SiO₂	205	5.67	203	5.64
ZrO₂	228	5.23	228	5.24

edge of the LMCT transitions of pure tetragonal zirconia is ∼5.2 eV, which is 0.5 eV lower than that of the ZrO₂/SiO₂ samples. For ZrO₂−SiO₂ mixed oxides, it was shown[5] that the highest absorption edge for the LMCT transitions is observed at the lowest zirconia content (3.9% ZrO₂) because of isolated extremely small zirconium oxide species in the silica matrix, and the absorption edge red shifts with increasing zirconia content because of the formation of bulk zirconia (tetragonal and monoclinic phases). Therefore, for the 1−15% ZrO₂/SiO₂ supported oxides, the UV−vis DRS results demonstrate that no bulklike zirconium oxide phases are present on the silica surface, in agreement with the Raman results.

Although the band maxima and edge energies of the ZrO₂/SiO₂ samples remain constant irrespective of environmental conditions, their band intensities markedly change upon hydration/dehydration (see Figure 7), which demonstrates that different zirconium oxide species with different absorption coefficients are present under hydrated and dehydrated conditions. This result suggests that the polymerization degree and/or coordination geometry of the Zr cations on silica may not change upon hydration/dehydration, but the ligands around the Zr cations (e.g., the ratio of Zr−OH to Zr−O−Si bonds) may be different, contributing to the difference in the absorption coefficient. In contrast, only a minor change in the band intensity for crystalline tetragonal ZrO₂ is observed upon hydration/dehydration.

In the corresponding NIR region (Figure 8) where the combination and overtone vibrations of O−H and C−H groups are located, the 7315 cm⁻¹ band due to the isolated Si−OH hydroxyls[23] decreases with increasing zirconia loading, indicating that the deposition of zirconium oxide species consumes the surface Si−OH groups to form Zr−O−Si bridging bonds. Pure tetragonal ZrO₂ exhibits two very weak bands at 7392 and 7194 cm⁻¹, which could be assigned to the overtone vibrations of bridging and terminal hydroxyls on the zirconia surface.[31] However, it

(31) Yamagushi, T.; Nakano, Y.; Tanabe, K. *Bull. Chem. Soc. Jpn.* **1978**, *51*, 2482.
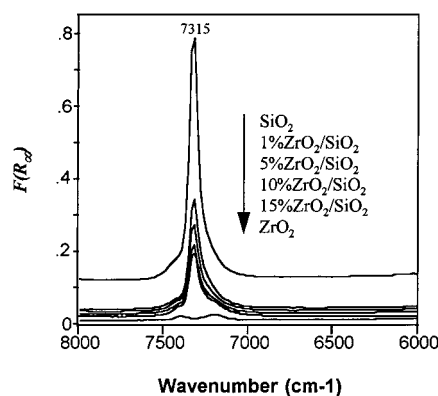
Figure 8. NIR DRS spectra of the dehydrated ZrO₂/SiO₂ samples.
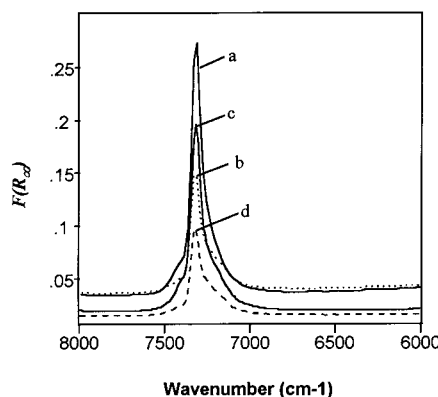
Figure 9. NIR DRS spectra of dehydrated (a) 5% ZrO₂/SiO₂ and (b) 5% V₂O₅/5%ZrO₂/SiO₂ (dashed lines) and (c) 15% ZrO₂/SiO₂ and (d) 5% V₂O₅/15% ZrO₂/SiO₂ (solid lines).

is not possible to identify the Zr−OH hydroxyls on the ZrO₂/SiO₂ supports because the 7315 cm⁻¹ band due to the isolated Si−OH hydroxyls is very intense.

Upon deposition of vanadium oxide species on ZrO₂/SiO₂ supports, the intensity of the 7315 cm⁻¹ band further decreases (see Figure 9), indicating that surface vanadium oxide species also interact with the silica surface, in agreement with the Raman results. However, the degree of interaction between surface vanadium oxide and zirconium oxide species appears to be higher at a higher zirconia loading because the amount of isolated Si−OH hydroxyls consumed by vanadium oxide is lower at a higher zirconia loading.

The UV−vis DRS spectra of the hydrated and dehydrated 5% V₂O₅/5% ZrO₂/SiO₂ and 5% V₂O₅/15% ZrO₂/SiO₂ samples are compared with the 5% V₂O₅/SiO₂ sample in Figure 10, and their band maxima and edge energies as well as those for the 5% V₂O₅/ZrO₂ and 10% V₂O₅/15% ZrO₂/SiO₂ samples are provided in Table 3. It is noted that the LMCT band of the V₂O₅/SiO₂ sample is much stronger than that of the ZrO₂/SiO₂ support with a similar loading, and the edge energy of the V₂O₅/SiO₂ sample is significantly lower than that of the ZrO₂/SiO₂ support. Thus, the spectral features and edge energies of the V₂O₅/ZrO₂/SiO₂ samples are mainly determined by the surface vanadium oxide species rather than zirconium oxide species. The dehydrated V₂O₅/ZrO₂/SiO₂ samples exhibit only one LMCT band, which apparently originates from the overlapped LMCT transitions of both V and Zr cations (electronic transitions from orbitals mainly consisting of oxygen 2p orbitals to vanadium 3d orbitals and zirconium 4d orbitals). The spectral features of the dehydrated V₂O₅/ZrO₂/SiO₂ samples are very similar to that of the dehy-

Table 3. Band Maxima and Edge Energies of 5% V$_2$O$_5$ on SiO$_2$, ZrO$_2$/SiO$_2$, and ZrO$_2$ Supports under Hydrated and Dehydrated Conditions

sample	band max (nm) (dehy)	E_g (eV) (dehy)	band max (nm) (hydr)	E_g (eV) (hydr)
5% V$_2$O$_5$/SiO$_2$	286	3.5	285, 433	2.4
5% V$_2$O$_5$/5% ZrO$_2$/SiO$_2$	296	3.4	299, 416	2.6
5% V$_2$O$_5$/15% ZrO$_2$/SiO$_2$	272	3.6	278, 404	3.1
10% V$_2$O$_5$/15% ZrO$_2$/SiO$_2$	281	3.4	271, 398	2.7
5% V$_2$O$_5$/ZrO$_2$	228, 320	3.0	228, 300, 402	2.8
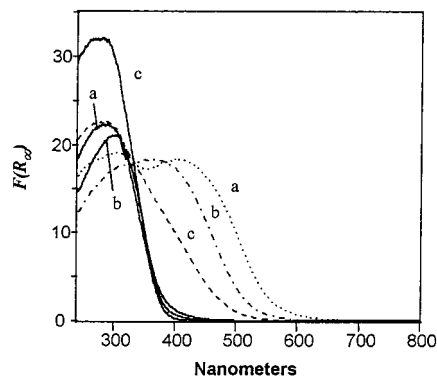
Figure 10. Comparison of UV–vis DRS spectra of (a) 5% V$_2$O$_5$/SiO$_2$, (b) 5% V$_2$O$_5$/5% ZrO$_2$/SiO$_2$, and (c) 5% V$_2$O$_5$/15% ZrO$_2$/SiO$_2$ in hydrated (dashed lines) and dehydrated (solid lines) conditions.

drated V$_2$O$_5$/SiO$_2$ sample, and their edge energies are about the same (3.4–3.6 eV). These results strongly suggest that the dehydrated surface vanadium oxide species on ZrO$_2$/SiO$_2$ supports are predominantly isolated VO$_4$ species, in analogy to the dehydrated V$_2$O$_5$/SiO$_2$ catalyst.[27] In contrast, the edge position of the dehydrated 5% V$_2$O$_5$/ZrO$_2$ sample is located at a lower energy of 3.0 eV with a band maximum at 320 nm (see Table 3), suggesting the presence of some polymerized vanadium oxide species on pure zirconia, which is consistent with the literature results.[16]

Upon hydration, two major LMCT bands (299–271 and 398–416 nm) are observed for these V$_2$O$_5$/ZrO$_2$/SiO$_2$ samples and their absorption edge shifts to lower energy, similar to the behavior of the 5% V$_2$O$_5$/SiO$_2$ sample. However, the edge energies of the hydrated 5% V$_2$O$_5$/ZrO$_2$/SiO$_2$ samples are substantially higher than those of the hydrated 5% V$_2$O$_5$/SiO$_2$ sample, especially at 15% ZrO$_2$ loading. In addition, the relative intensity of the LMCT band at 398–416 nm decreases significantly with increasing zirconia content (see Figure 10). The hydrated surface vanadium oxide species on silica have been shown to consist of chain and/or two-dimensional polymerized VO$_5$/VO$_6$ units.[27] It appears that the presence of zirconium oxide species on silica modifies the molecular structure of the hydrated surface vanadium oxide species and significantly decreases their polymerization degree relative to the hydrated V$_2$O$_5$/SiO$_2$. For the hydrated 5% V$_2$O$_5$/ZrO$_2$ sample (see Table 3), two LMCT bands of the V(V) cations are also observed at 300 and 402 nm (the 228 nm band is due to the bulk ZrO$_2$) with an edge energy of 2.8 eV. In the hydrated state, the zirconia surface at monolayer coverage of vanadia is known to be dominated by decavanadate clusters (V$_{10}$O$_{28}$).[16] Therefore, the higher edge energy of 3.1 eV for the hydrated 5% V$_2$O$_5$/15% ZrO$_2$/SiO$_2$ sample suggests that the polymerization degree of the surface vanadium oxide species on 15% ZrO$_2$/SiO$_2$ support might be even lower than 10 V atoms.

4. TPR. TPR experiments were performed on pure ZrO$_2$ as well as on dispersed ZrO$_2$/SiO$_2$ supports, and no noticeable H$_2$ consumption was observed for these samples. Thus, the H$_2$ consumption detected for various V$_2$O$_5$/ZrO$_2$/
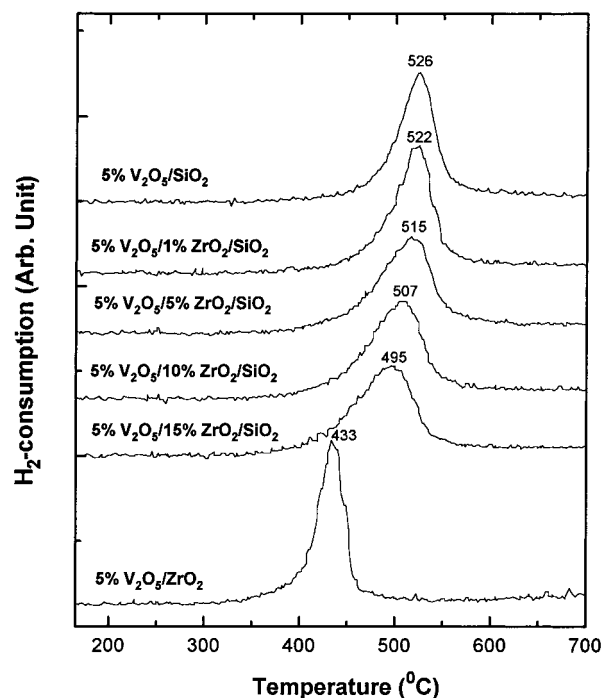
Figure 11. Comparison of TPR profiles of 5% V$_2$O$_5$ on SiO$_2$, ZrO$_2$/SiO$_2$, and ZrO$_2$ supports.

Table 4. Comparison of TPR Results of 5% V$_2$O$_5$ on SiO$_2$, ZrO$_2$/SiO$_2$, and ZrO$_2$ Supports (Sample Weight ∼ 60 mg, Temperature Rate = 10 °C/min)

sample	T_{onset} (°C)	T_{max} (°C)	fwhm (°C)	H/V (atomic ratio)
5% V$_2$O$_5$/SiO$_2$	383	526	40	1.88
5% V$_2$O$_5$/1% ZrO$_2$/SiO$_2$	373	522	43	2.03
5% V$_2$O$_5$/5% ZrO$_2$/SiO$_2$	365	515	61	2.00
5% V$_2$O$_5$/10% ZrO$_2$/SiO$_2$	341	507	60	1.87
5% V$_2$O$_5$/15% ZrO$_2$/SiO$_2$	338	495	69	1.92
5% V$_2$O$_5$/ZrO$_2$	315	433	30	1.87

SiO$_2$ catalysts primarily originates from the reduction of the surface vanadium oxide species.

The TPR spectra of 5% V$_2$O$_5$ on various supports (SiO$_2$, ZrO$_2$/SiO$_2$, and ZrO$_2$) are shown in Figure 11, and the corresponding TPR results are listed in Table 4. It can be seen that both the initial (T_{onset}) and maximum (T_{max}) reduction temperatures of the 5% V$_2$O$_5$/ZrO$_2$/SiO$_2$ catalysts decrease systematically with increasing zirconia content, suggesting that the reducibility of the surface vanadium oxide species on the ZrO$_2$/SiO$_2$ support increases because of the interaction between the surface vanadium oxide and zirconium oxide species. However, the 5% V$_2$O$_5$/ZrO$_2$/SiO$_2$ samples possess much lower reducibilities than the 5% V$_2$O$_5$/ZrO$_2$ sample, which suggests that silica as a substrate plays an important role in modifying the chemical properties of the zirconium oxide species. A similar reducibility trend is also observed for the 10% V$_2$O$_5$/ZrO$_2$/SiO$_2$ samples, as shown in Table 5. Both T_{onset} and T_{max} decrease with increasing zirconia content,

Table 5. Comparison of TPR Results of 10% V₂O₅ on SiO₂ and ZrO₂/SiO₂ Supports (Sample Weight ∼ 60 mg, Temperature Rate = 10 °C/min)

sample	T_{onset} (°C)	T_{max} (°C)	fwhm (°C)	H/V (atomic ratio)
10% V₂O₅/SiO₂	390	540	38	2.00
10% V₂O₅/1% ZrO₂/SiO₂	382	530	42	1.95
10% V₂O₅/5% ZrO₂/SiO₂	353	530	49	1.93
10% V₂O₅/10% ZrO₂/SiO₂	355	521	50	1.93
10% V₂O₅/15% ZrO₂/SiO₂	344	518	54	1.90

indicative of the increased reducibility of the surface vanadium oxide species relative to the 10% V₂O₅/SiO₂ catalyst.

The H₂ consumption represented as H/V ratios for both 5% and 10% V₂O₅ loading samples on the different supports is almost constant at ∼2 (see Tables 4 and 5), indicating that the average oxidation state of the V cations on these supports after TPR runs up to 700 °C is about +3. Moreover, the reduction peak widths of the V₂O₅/ZrO₂/SiO₂ samples are much broader than either V₂O₅/SiO₂ or V₂O₅/ZrO₂ at the same vanadia loading and generally increase with zirconia loading up to 15% ZrO₂. This trend suggests that there exists a distribution of surface vanadium oxide species on the ZrO₂/SiO₂ supports with different reducibilities (e.g., VO₄ species with different oxygenated ligands).

5. Methanol Oxidation. Methanol oxidation was used to examine the catalytic properties of the ZrO₂/SiO₂ and V₂O₅/ZrO₂/SiO₂ catalysts. The silica support did not show any noticeable activity for methanol oxidation under the present experimental conditions. The catalytic results of the ZrO₂/SiO₂ supported oxides for methanol oxidation at 270 and 290 °C are presented in Tables 6 and 7. Pure ZrO₂ produces exclusively methyl formate (MF) and CO, which is due to its special surface characteristics (i.e., coexistence of redox sites and acid/basic sites).[15] The surface zirconium oxide species on silica exhibit catalytic properties different from those of pure ZrO₂. MF production is significantly reduced; instead, 20−49% formaldehyde and 4−23% dimethyl ether (DME) are obtained, depending on the reaction temperature and the ZrO₂ loading. It has been proposed[32] that increasing the nucleophilic character (or basicity) of the oxygen species on the catalyst usually increases the production of MF and carbon oxides. The production of DME indicates the presence of the acid sites. These catalytic results suggest that the basicity/acidity of zirconium oxide is modified by the silica substrate and that the oxygen species on ZrO₂/SiO₂-supported oxides are less basic and more acidic than those on pure ZrO₂.

The TOFs for methanol oxidation over ZrO₂/SiO₂ catalysts decrease with increasing zirconia loading. The oxidizing potential of the Zr cations on silica appears to be higher than that of pure ZrO₂ and is inversely proportional to the zirconia loading, which is more evident from the activity values obtained at 290 °C. Increasing the reaction temperature from 270 to 290 °C significantly increases the overall activity of the ZrO₂/SiO₂-supported oxides by over 2 times, whereas the activity of pure ZrO₂ only slightly increases. These results demonstrate that the catalytic properties of the surface zirconium oxide species are strongly modified by the interaction with the SiO₂ support.

The catalytic results of the surface vanadium oxide species on the SiO₂, ZrO₂, and ZrO₂/SiO₂ supports for methanol oxidation at 270 and 250 °C are provided in Tables 8 and 9. All of the V₂O₅-based catalysts exhibit

(32) Tatibouët, J. M. *Appl. Catal. A* **1997**, *148*, 213.

higher selectivity to formaldehyde (>65%), and the MF production is greatly suppressed (<30%). For the V₂O₅/ZrO₂/SiO₂ catalysts with high vanadia loadings (≥5% V₂O₅), the selectivity of MF is even less than 5%. Interestingly, the activity of the 1% V₂O₅/SiO₂ sample at 270 °C (A_c ∼ 1 mmol/g·h) is lower than that of the 1% ZrO₂/SiO₂ sample (A_c ∼ 4 mmol/g·h) (see Tables 6 and 8), demonstrating that the zirconium oxide species on silica possess a higher reactivity for methanol oxidation than the isolated VO₄ species on silica. However, when 1% V₂O₅ is deposited on 1% ZrO₂/SiO₂, the overall activity increases by about 4 times (A_c ∼ 19 mmol/g·h), suggesting that the enhanced reactivity is associated with the direct interaction of the surface vanadium oxide species with the surface zirconium oxide species on silica. In addition, the overall activity of the 1% V₂O₅/ZrO₂/SiO₂ catalysts significantly increases with the zirconia content. Thus, the activity enhancement and selectivity pattern of V₂O₅/ZrO₂/SiO₂ catalysts suggest that the surface V cations serve as the active sites for methanol oxidation, and the degree of interaction between the surface vanadium oxide and zirconium oxide species on silica increases with the zirconia content.

Furthermore, the methanol oxidation TOF of the V₂O₅/ZrO₂/SiO₂ catalysts generally increases with the zirconia content but decreases with increasing vanadia content (see Tables 8 and 9). The activities (TOFs) of the V₂O₅/ZrO₂/SiO₂ catalysts are 1−2 orders of magnitude higher than that of the V₂O₅/SiO₂ catalyst, depending on both vanadia and zirconia concentrations. These results strongly suggest that the surface vanadium oxide species directly interact with the zirconium oxide species on silica. However, all of the ZrO₂/SiO₂ supports are significantly less active than pure ZrO₂ as supports for vanadium oxide during methanol oxidation, which may be due to the modified chemical properties of the zirconium oxide species on silica as well as the presence of some V−O−Si bonds besides V−O−Zr bonds.

Discussion

Structural Characteristics and Catalytic Properties of the Highly Dispersed ZrO₂/SiO₂-Supported Oxides. The combined Raman, UV−vis DRS, and XPS results strongly suggest that the zirconium oxide species on silica are highly dispersed, and their molecular structure is sensitive to the environmental condition (e.g., different Zr−OH to Zr−O−Si bond ratios). XPS surface analysis shows that the Zr/Si atomic ratio increases almost linearly with the zirconia content up to 15% ZrO₂, demonstrating a high dispersion from 1% to 15% ZrO₂. No apparent bulk zirconia phase (amorphous, tetragonal, cubic, or monoclinic) was detected by Raman spectroscopy. Instead, a weak Raman band at 940∼950 cm⁻¹ due to the Zr−O−Si bridging bonds is observed for the dehydrated samples. The consumption of surface Si−OH hydroxyls by the dispersed zirconia oxide species is confirmed by NIR DRS measurements, consistent with the formation of Zr−O−Si bonds. Upon hydration of the dehydrated ZrO₂/SiO₂ samples, the Raman band centered at 975−980 cm⁻¹ becomes more intense and broader, suggesting that some surface Si−OH and Zr−OH hydroxyls are generated from the hydrolysis of Zr−O−Si bridging bonds. This is further confirmed by the UV−vis DRS results, which show that the ligands of the Zr cations may be different upon hydration/dehydration.

In addition, the UV−vis DRS and XPS characterization data suggest that in the dehydrated state the same type

Table 6. Activity/Selectivity of ZrO₂/SiO₂ Catalysts for Methanol Oxidation at 270 °C

catalyst	$A_c{}^a$ (mmol/g·h)	TOF[b] (10^{-3} s^{-1})	selectivity (%) HCHO	MF	DMM	DME	CO
1% ZrO₂/SiO₂	4	13					
5% ZrO₂/SiO₂	11	7	32	52	7	9	0
10% ZrO₂/SiO₂	9	3	33	40	8	19	0
15% ZrO₂/SiO₂	8	2	20	49	8	23	0
ZrO₂	10		0	100	0	0	0

[a] Millimoles of methanol converted per gram of catalyst per hour. [b] TOF is calculated on the basis of the total Zr atoms in the catalysts for the production of HCHO (formaldehyde) + MF (methyl formate) + DMM (dimethoxymethane).

Table 7. Activity/Selectivity of ZrO₂/SiO₂ Catalysts for Methanol Oxidation at 290 °C

catalyst	A_c (mmol/g·h)	TOF[b] (10^{-3} s^{-1})	selectivity (%) HCHO	MF	DMM	DME	CO
1% ZrO₂/SiO₂	14	46	49	45	2	4	0
5% ZrO₂/SiO₂	28	18	45	45	3	7	0
10% ZrO₂/SiO₂	29	8	26	51	3	10	10
15% ZrO₂/SiO₂	26	5	33	43	2	12	10
ZrO₂	14		0	70	0	0	30

[a] TOF is calculated on the basis of the total V atoms in the catalysts for the production of HCHO (formaldehyde) + MF (methyli formate) + DMM (dimethoxymethane).

Table 8. Activity and Selectivity of 1% V₂O₅/SiO₂ and V₂O₅/ZrO₂/SiO₂ Catalysts for Methanol Oxidation at 270 °C

catalyst	A_c (mmol/g·h)	TOF[a] (10^{-3} s^{-1})	selectivity (%) HCHO	MF	DMM	DME	HCHO
1% V₂O₅/SiO₂	1	2					
1% V₂O₅/1% ZrO₂/SiO₂	19	45	78	8	8	6	78
1% V₂O₅/5% ZrO₂/SiO₂	37	87	75	14	5	6	75
1% V₂O₅/10% ZrO₂/SiO₂	64	154	66	27	2	5	66
5% V₂O₅/5% ZrO₂/SiO₂	73	33	81	6	2	11	81
5% V₂O₅/10% ZrO₂/SiO₂	154	72	84	5	4	7	84
10% V₂O₅/10% ZrO₂/SiO₂	133	31	82	3	6	9	82

[a] TOF is calculated on the basis of the total V atoms in the catalysts for the production of HCHO (formaldehyde) + MF (methyl formate) + DMM (dimethoxymethane).

Table 9. Activity and Selectivity of 1% V₂O₅/ZrO₂ and V₂O₅/ZrO₂/SiO₂ Catalysts for Methanol Oxidation at 250 °C

catalyst	A_c (mmol/g·h)	TOF (10^{-3} s^{-1})	selectivity (%) HCHO	MF	DMM	DME
1% V₂O₅/1% ZrO₂/SiO₂	9	23	77	10	13	0
1% V₂O₅/5% ZrO₂/SiO₂	18	43	74	7	14	5
1% V₂O₅/10% ZrO₂/SiO₂	33	80	71	16	8	5
5% V₂O₅/5% ZrO₂/SiO₂	40	18	78	4	8	10
5% V₂O₅/10% ZrO₂/SiO₂	73	34	76	4	13	7
10% V₂O₅/10% ZrO₂/SiO₂	77	18	77	0	14	9
10% V₂O₅/15% ZrO₂/SiO₂	106	25	84	0	9	7
1% V₂O₅/ZrO₂	401	988	69	26	2	3

of surface zirconium oxide species is present on silica regardless of zirconia loading up to 15% ZrO₂. The BE value of Zr 3d$_{5/2}$ obtained by XPS measurements is constant at 182.3 eV. The band maxima and edge energies of the LMCT transitions are the same. These results suggest that the molecular structure and/or the polymerization degree of the zirconium oxide species are very similar, independent of the zirconia loading.

All of the literature results indicate that the Zr(IV) cations that interact with SiO₂ possess a coordination higher than 4. For ZrO₂–SiO₂ glasses, various coordination geometries around Zr(IV) cations have been reported, depending on the chemical composition and preparation method. Bihuniak et al.[33] suggested that Zr(IV) cations are 7- or 8-fold-coordinated, based on the Raman and IR spectral analysis and the refractivity dependence on the zirconia concentration. However, EXAFS experiments[7,34]

indicated that at low zirconia contents (ZrO₂ ≤ 20%) the Zr(IV) cations are in 5-fold coordination, and both Zr–OH (2 or 1) and Zr–O–Si (3 or 4) bonds are present around the Zr coordination sphere.[7] For the 9.3 wt % ZrO₂–SiO₂ mixed oxide catalyst, a coordination of 4.5 was reported by Moon et al.[5] on the basis of their EXAFS analysis. Moreover, many Zr(IV)- and Si(IV)-containing compounds usually consist of 6–8-fold-coordinated Zr(IV) cations, e.g., Na₂ZrSi₃O₉·2H₂O (6-fold), Na₂ZrSi₄O₁₁ (6-fold), Na₂ZrSi₆O₁₅·3H₂O (6-fold), ZrSiO₄ (8-fold), and K₂ZrSi₃O₉ (6-fold).[7] Therefore, it is reasonable to speculate that the coordination of the surface Zr cations on silica should be 5-fold or higher. Unfortunately, no structural characterization data on the coordination geometry of the surface Zr cations on silica are presently available in the literature. It is also not possible to derive a detailed molecular structure for the ZrO₂/SiO₂-supported oxides from the results obtained by the present characterization techniques. Further investigations using structural characterization techniques more specific to Zr atoms (e.g., XANES and EXAFS spectroscopies) are necessary to

(33) Bihuniak, P. P.; Condrate, R. A. *J. Non-Cryst. Solids* **1981**, *44*, 331.

(34) Osuka, T.; Morikawa, H.; Marumo, F.; Tohji, K.; Udagawa, Y.; Yasumori, A.; Yamane, M. *J. Non-Cryst. Solids* **1986**, *82*, 154.

clarify the coordination geometry of the surface Zr cations on silica.

The methanol oxidation results indicate that the highly dispersed ZrO_2/SiO_2-supported oxides exhibit catalytic properties different from those of pure ZrO_2. The zirconium oxide species on silica appear to be more active than pure ZrO_2, and their selectivities are quite different. Pure ZrO_2 produces exclusively MF and CO. For the ZrO_2/SiO_2-supported oxides, the MF production is markedly reduced, and some formaldehyde and dimethyl ether are produced. These catalytic results suggest that the oxygen species on ZrO_2/SiO_2-supported oxides are less basic than those on pure ZrO_2, and some acid sites are generated because of the strong interaction between zirconium oxide species and silica (Zr−O−Si chemical bonding). This is reasonable considering that Si(IV) cations are more electronegative (more electron withdrawn) than Zr(IV) cations,[35] which results in a lower electron density around oxygen atoms on ZrO_2/SiO_2-supported oxides because of the formation of Zr−O−Si bonds.

The TOF of the ZrO_2/SiO_2-supported oxide decreases with increasing zirconia loading, indicating that the average reactivity of the Zr sites is a strong function of zirconia loading. This fact suggests that the local structure and/or the polymerization degree of the Zr cation is dependent on the zirconia coverage on silica, as in the case of highly dispersed TiO_2/SiO_2-supported oxides.[23] This is contradictory to the spectroscopic characterization results, which suggest that the same type of the zirconium oxide species is present on silica at 1−15% ZrO_2 loadings. Naito et al. reported[10] that the highly dispersed ZrO_2/SiO_2-supported oxides behave very differently from pure zirconia in propene hydrogenation; however, their initial specific rates are independent of the zirconia content on silica up to 16% ZrO_2. They proposed that a 2D network of zirconium oxide species is present on the silica surface. A possible explanation to the above conflicting conclusions from the different techniques in the present work may be that in the 1−15% ZrO_2 loading region the XPS and UV−vis DRS techniques are not sensitive enough to detect small changes in the local structure of the Zr cations on silica (e.g., different Zr−OH/Zr−O−Si to Zr−O−Zr ratios).

Structural Characteristics and Catalytic Properties of the Highly Dispersed $V_2O_5/ZrO_2/SiO_2$ Catalysts. Unlike the $V_2O_5/TiO_2/SiO_2$ catalyst system, no studies have previously been performed on the similar $V_2O_5/ZrO_2/SiO_2$ catalyst system. As discussed below, the structural characteristics and catalytic properties of the surface vanadium oxide species on the ZrO_2/SiO_2 supports are very similar to those on the TiO_2/SiO_2 supports.[36] The in situ Raman and UV−vis−NIR DRS spectroscopies indicate that the surface vanadium oxide species on the highly dispersed ZrO_2/SiO_2 supports are sensitive to the environmental conditions. In the hydrated state, the Raman spectra of the highly dispersed $V_2O_5/ZrO_2/SiO_2$ catalysts are very similar to those of the highly dispersed V_2O_5/SiO_2 catalysts, which possess polymerized VO_5/VO_6 species.[27] The UV−vis DRS results indicate that the polymerization degree of the VO_5/VO_6 species on the ZrO_2/SiO_2 supports is lower than that on pure silica, which is probably because of the presence of somewhat more basic zirconium oxide species. However, the catalysts are usually operated in the dehydrated state during methanol oxidation as well as the TPR studies. Therefore, the structural characteristics of the catalysts in the dehydrated state

are more relevant to the chemical and catalytic properties of the catalysts. Consequently, only the dehydrated molecular structures of the $V_2O_5/ZrO_2/SiO_2$ catalysts are addressed below.

In the dehydrated state, the spectral features and edge energies of the LMCT transitions for the highly dispersed $V_2O_5/ZrO_2/SiO_2$ catalysts are very close to those of the highly dispersed V_2O_5/SiO_2, suggesting that isolated VO_4 units (i.e., O=V(O−support)₃ group) are dominant on the ZrO_2/SiO_2 supports. The Raman spectra of the highly dispersed $V_2O_5/ZrO_2/SiO_2$ catalysts are also very similar to those of the highly dispersed V_2O_5/SiO_2 with the exception of the Raman band at 915−930 cm⁻¹, which grows in intensity with both vanadia and zirconia loadings. This Raman band is not due to crystalline zirconium vanadate (ZrV_2O_7), which exhibits a strong Raman band at ∼780 cm⁻¹,[22,37] but it might be associated with the polymerized surface vanadium oxide species that display a Raman band at 840−940 cm⁻¹ on pure ZrO_2.[16] However, no apparent additional band appears at 200−300 cm⁻¹ because of the V−O−V bending mode.[30] In addition, the UV−vis DRS results indicate that the surface vanadium oxide species on the ZrO_2/SiO_2 supports are predominantly isolated VO_4 species, which possess edge energy and spectral features similar to those of the highly dispersed V_2O_5/SiO_2 catalysts. It has been shown that for the dehydrated 1% V_2O_5/Al_2O_3 sample where the isolated VO_4 species are dominant a strong, broad Raman band was observed at 840−940 cm⁻¹ and was assigned to the VO_3 stretching functionalities.[30] Thus, the strong, broad Raman band observed at 915−930 cm⁻¹ for the $V_2O_5/ZrO_2/SiO_2$ catalysts at higher zirconia loading is probably due to the isolated VO_4 species, with the VO_3 vibration becoming more Raman active in association with the replacement of the $Si^{IV}O^-$ ligands by $Zr^{IV}O^-$ ligands.

NIR DRS experiments demonstrate that the deposition of vanadium oxide on ZrO_2/SiO_2 also consumes the surface Si−OH hydroxyls, indicative of the formation of V−O−Si bridging bonds. Furthermore, it is noted that all of the TPR peaks observed for the highly dispersed $V_2O_5/ZrO_2/SiO_2$ catalysts are broad and unresolvable, and their T_{onset} and T_{max} are located between those of V_2O_5/SiO_2 and V_2O_5/ZrO_2 catalysts. These results suggest that although the surface vanadium oxide species are predominantly isolated VO_4 units on the ZrO_2/SiO_2 surface, the V(V) cations most likely possess different $Zr^{IV}O^-$ to $Si^{IV}O^-$ ligand ratios with varying reducibilities that depend on zirconia and vanadia concentrations on silica.

Even far below the monolayer coverage for either vanadium oxide or zirconium oxide on silica, the addition of 1% V_2O_5 onto the 1% ZrO_2/SiO_2 sample greatly enhances the overall activity (by a factor of 4) for methanol oxidation. This result suggests a direct interaction between the surface vanadium oxide and zirconium oxide species (i.e., the formation of V−O−Zr connections) and indicates that the V(V) cations are preferentially coordinated to the surface zirconium oxide species. This preferential interaction may be associated with the preparation process where the surface Zr−OH hydroxyls or hydroxyls around the Zr cations could be more reactive than other surface Si−OH hydroxyls with V isopropoxide precursor molecules.

Although the molecular structure of the highly dispersed $V_2O_5/ZrO_2/SiO_2$ catalysts in the dehydrated state is pretty much the same as that of the highly dispersed V_2O_5/SiO_2 catalysts, the modification of the silica support by the surface zirconium oxide species greatly affects the catalytic

(35) Sanderson, R. T. *J. Chem. Educ.* **1988**, *65*, 113.
(36) Gao, X.; Bare, S. R.; Fierro, J. L. G.; Wachs, I. E. *J. Phys. Chem. B* **1998**, *103*, in press.

(37) Sanati, M.; Andersson, A.; Wallenberg, L. R.; Rebenstorf, B. *Appl. Catal. A* **1993**, *106*, 51.

properties of the supported vanadium oxide. The TOFs for methanol oxidation on the highly dispersed $V_2O_5/ZrO_2/SiO_2$ supports increase by 1−2 orders of magnitude relative to the V_2O_5/SiO_2 catalysts. The replacement of the $Si^{IV}O^-$ ligand by the $Zr^{IV}O^-$ ligand in the coordination sphere of the V cation enhances its specific activity. Therefore, the formation of V−O−Zr bonds in the isolated vanadium oxide species on the ZrO_2/SiO_2 support is responsible for the enhanced reactivity of the surface V active sites.

The basis for this support effect may lie in the increase of the electron density of the bridging oxygen in the V−O−Zr bonds relative to the V−O−Si bonds because the Zr-(IV) cations possess a lower electronegativity than the Si(IV) cations.[35] However, the electronegativity of the Zr-(IV) cations that interact with both silica and vanadium oxide species should be higher than that of Zr(IV) in pure ZrO_2 because of the higher electron-withdrawing ability of Si(IV) and V(V) cations. Therefore, the influence of silica as the substrate reduces the electron density of the oxygen atom in the V−O−Zr bridging bond, which may partially contribute to the decreased reactivity of the surface V sites during methanol oxidation relative to V_2O_5/ZrO_2.

Conclusions

Highly dispersed ZrO_2/SiO_2 and $V_2O_5/ZrO_2/SiO_2$ catalysts were successfully synthesized and investigated by in situ Raman and UV−vis−NIR DRS spectroscopies, as well as XPS. These characterization techniques demonstrated that both zirconium oxide and vanadium oxide species are highly dispersed on silica, and their surface structures are sensitive to environmental conditions. The surface zirconium oxide species on silica are the same type up to 15% ZrO_2 loading. The Zr−O−Si bridging bonds are observed on the dehydrated ZrO_2/SiO_2 samples and can be hydrolyzed into Zr−OH and Si−OH hydroxyls upon hydration. The surface vanadium oxide species on the highly dispersed ZrO_2/SiO_2 supports are predominantly isolated VO_4 units in the dehydrated state. Upon hydration, the surface vanadium oxide species are polymerized, and the degree of polymerization depends on both vanadia and zirconia loadings. The surface V cations preferentially interact with the zirconium oxide species on the silica surface. Consequently, the reducibility and catalytic properties of the surface vanadium oxide species are significantly affected. The TOFs of the surface VO_4 species on ZrO_2/SiO_2 supports for methanol oxidation increase by 1−2 orders of magnitude relative to the V_2O_5/SiO_2 catalysts. On the basis of the structural characterization data and catalytic results, it is concluded that the replacement of $Si^{IV}O^-$ oxygenated ligands by less electronegative $Zr^{IV}O^-$ ligands around the V cations is responsible for the enhanced reactivity of the V sites.